Development of an Electrophysiological Assay for Kv7 Modulators on IonWorks Barracuda

Benjamin Wilenkin,[1] Kevin D. Burris,[1] Brian J. Eastwood,[2] Emanuele Sher,[3] Andrew C. Williams,[4] and Birgit T. Priest[1]

Departments of [1]Quantitative Biology, [2]Statistics, [4]Medicinal Chemistry, and [3]Discovery Pain Group, Eli Lilly and Company, Indianapolis, Indiana.

ABSTRACT

Relief from chronic pain continues to represent a large unmet need. The voltage-gated potassium channel Kv7.2/7.3, also known as KCNQ2/3, is a key contributor to the control of resting membrane potential and excitability in nociceptive neurons and represents a promising target for potential therapeutics. In this study, we present a medium throughput electrophysiological assay for the identification and characterization of modulators of Kv7.2/7.3 channels, using the IonWorks Barracuda™ automated voltage clamp platform. The assay combines a family of voltage steps used to construct conductance curves with a unique analysis method. Kv7.2/7.3 modulators shift the activation voltage and/or change the maximal conductance of the current, and both parameters have been used to quantify compound mediated effects. Both effects are expected to modulate neuronal excitability in vivo. *The analysis method described assigns a single potency value that combines changes in activation voltage and maximal conductance and is expected to predict compound mediated changes in excitability.*

Keywords: Kv7, IonWorks Barracuda, KCNQ, automated electrophysiology

INTRODUCTION

Chronic pain should be considered a global epidemic, since as recent as 2011, it was estimated that 20% of adults suffer from pain, and another 1 in 10 are diagnosed with chronic pain every year.[1] Worldwide more than 1.5 billion people suffer from some form of chronic debilitating pain. Despite the large unmet need, adequate treatments are lacking. The development of novel classes of analgesics has largely been unsuccessful, and the most commonly prescribed drugs continue to be NSAIDS, opioids, antiepileptic drugs, and antidepressants. Especially in light of the rapidly growing incidence of opioid addiction and overdose,[2] there is an urgent need for safer analgesics without abuse potential.

Comprehensive research activities focused on ion channels expressed in primary sensory neurons have provided important learnings and potential targets for novel analgesics. A class of channel proteins that are of particular interest are the family of Kv7 potassium channels, encoded by the KCNQ1–5 genes. Kv7 channels are notable because they activate slowly, are non-inactivating, and are active at or near the resting membrane potential of neurons. These biophysical characteristics allow Kv7 channels to modulate neuronal excitability.[3–5] Kv7 channels are sometimes referred to as "M channels" because muscarinic cholinergic agonists reduce the corresponding currents through phospholipase C mediated hydrolysis of PIP_2.[6] This mechanism provides a direct link between G protein coupled receptors and a physiological K^+ current affecting excitability.[6–8]

Structurally, Kv7 channels are characterized by six transmembrane domains and a single pore loop and function as either hetero- or homotetramers.[9] Given their influence on resting membrane potential and neuronal excitability, it is not surprising that they have emerged as a promising target for the treatment of hyperexcitability-related disorders, such as neuropathic pain and epilepsy.[10]

Kv7.2–Kv7.5 subunits are expressed widely throughout the central and peripheral nervous system, as well as a number of other nonexcitable tissues.[11–15] In small diameter dorsal root ganglion (DRG) neurons, evidence from single cell PCR, immunocytochemistry, and pharmacologic studies supports heteromeric Kv7.2/7.3 channels as the main channel subtype,[14] whereas the M-current in most central nervous system neurons is most likely a combination of Kv7.2/7.3 and Kv7.3/7.5 channels.[15]

A number of Kv7 channel openers have been developed to treat hyperexcitability disorders.[16] Flupirtine (Katadolon™), a nonselective Kv7 opener (Kv7.2–7.5), has been used to treat acute and chronic pain in several European countries since the 1980s.[17] Flupirtine was withdrawn from the market in the EU in 2018 because of the occurrence of rare, but life threatening, liver injury. Retigabine, also known as ezogabine in the United States, is a close analog of flupirtine and was approved as an

 DOI: 10.1089/adt.2019.942

anticonvulsant in the United States (Potiga™) and in Europe (Trobalt™).[18] Retigabine was withdrawn from the market in 2017 because of severe side effects limiting its use.[16]

Since the initial clinical approvals of flupirtine and retigabine, numerous Kv7 activators have been developed. They fall into several categories with regard to their mechanism of channel activation and subtype selectivity. Retigabine and flupirtine do not affect Kv7.1 currents but are widely thought of as nonselective among Kv7.2–7.5 channel subtypes. Several researchers have demonstrated the importance of a tryptophan residue in transmembrane segment S5, namely Trp-265 (Kv7.3 numbering), for the activity of retigabine.[19,20] Trp-265 is conserved among Kv7.2–7.5 subunits. Mutation of the corresponding leucine residue in Kv7.1 to Trp resulted in a mutant channel that was sensitive to retigabine, although with a voltage-independent reduction of current amplitude as the dominant effect.[19,20] In contrast, Kv7.1 channels carrying transmembrane segment S6 from Kv7.2 were potentiated by retigabine, suggesting that additional amino acids are critical for the activity of retigabine. Through additional mutagenesis and modeling work, a binding/activity model has been developed in which retigabine binds by hydrogen bonding or π–π interaction to Trp-265, disrupting a π–π interaction between Trp-265 and other aromatic residues within S5 and S6 of the same subunit that in the absence of drug stabilize the closed state of the channel.[21,22] Retigabine may simultaneously contact residues in S6 of the adjacent subunit, further stabilizing the open state.[21]

Additional evidence placing the retigabine binding site within the pore comes from studies with "sensorless" channels, consisting only of the pore domains of Kv7.2 and Kv7.3. Single channel recordings of these constructs reconstituted into lipid bilayers showed that retigabine was able to stabilize the open state.[22] Furthermore, the relative potency for homomeric and heteromeric Kv7.2 and Kv7.3 channels and the dependence on Trp-265 were reproduced in these constructs lacking the voltage sensor domains.

The stoichiometry of retigabine binding to Kv7 channels remains to be fully elucidated. Work by Kim *et al.* using heteromeric Kv7.2/7.3 channels with Trp-265 mutations in either but not both subunits demonstrated intermediate effects of retigabine, suggesting that binding of four molecules of retigabine is necessary for maximal channel activation.[23] However, more recent work by Yau *et al.* claims that only a single retigabine molecule per channel is required to exert the full effect of the drug, based on the observation of biphasic conductance-voltage curves at intermediate retigabine concentrations.[24] It is possible that the discrepancy is related to the oocyte expression system, since biphasic curves were not seen in CHO cells by Wickenden *et al.*[25] or in our experiments with flupirtine.

Several other Kv7 modulators, including NS15370, GABA, gabapentin, and SCR2682,[26–29] also appear to bind within the pore domain.

Other Kv7 modulators do not require Trp-265 for activity. This group includes ICA-27243 and ICA-069673.[30,31] Notably, these compounds display some selectivity among Kv7.2–7.5 subtypes. ICA-27243 is a potent modulator of Kv7.2/7.3 channels, at least 10-fold selective over Kv7.4 and essentially inactive at Kv7.3/7.5 or Kv7.3 homomers.[30,32] Work by several groups has indicated the importance of residues in the voltage sensor domain and particularly in S3 for the activity of these types of Kv7 modulators.[30,31] In support of a binding site within the voltage sensor domain, binding of four molecules of ICA-069673 per channel was required for full activity.[33] The exact mechanism and nature of the residues involved in the interaction remain to be determined.

ML213 is closely related to ICA-27243 and ICA-069673, but lacks selectivity among Kv7.2–7.5 channels and appears to interact with Trp-265.[23,34] SMB-1 binds to the same site as retigabine but exerts opposite effects on Kv7.2 and Kv7.4 channels and features a carbonyl oxygen in the center of the molecule, similar to the Icagen compounds and ML-213 and distinct from retigabine.[35]

Clearly the relationship among structure, binding site, and subtype selectivity is complicated. A high-throughput electrophysiology assay combined with extensive investigation of structure-activity relationships (SARs) and profiling on different Kv7 subtypes should help to shed light on the factors involved. In this article, we introduce such an assay on the IonWorks Barracuda™ (Molecular Devices, Sunnyvale, CA) platform. The assay provides information on $V_{0.5}$ shifts and changes in maximal conductance. These distinctions are important in understanding the mechanism of channel activation and guiding SAR efforts. Despite the differences in the way different compounds activate Kv7 channels, all appear to restore Kv7 currents near the activation threshold following PIP_2 depletion and rises in intracellular calcium concentration. Furthermore, retigabine and flupirtine hyperpolarized DRG neurons after receptor-mediated depolarization.[36] These findings support the idea of comparing channel activators by the concentration required to increase current near the foot of the activation curve.[37–43]

MATERIALS AND METHODS

Reagents

Doxycycline and ML252 were purchased from Sigma-Aldrich (St. Louis, MO). Flupirtine maleate was from Selleckchem (Houston, TX), and dimethyl sulfoxide (DMSO) was obtained from Fisher Scientific (Hampton, NH). 3,3-Dimethylbutanoic Acid (6-Trifluoromethoxy-3-methyl-3H-

benzothiazol-2-ylidine) hydrazide (hereon referred to as benzothiazolone hydrazone) and N-(6-chloro-pyridin-3-yl)-3,4-difluoro-benzamide (hereon referred to as ICA-27243) were synthesized in house based on published structures.[32,44]

Cell Culture

HEK293 cells expressing heteromeric human Kv7.2/3 and Kv7.3/5 channels were obtained from ChanTest Corp./Charles River Laboratories (Cat Nos. CT6147 and CT6018, respectively). In these cell lines, expression of Kv7.3 is constitutive, whereas expression of Kv7.2 or Kv7.5 is inducible by exposure to tetracycline/doxycycline. Cells were maintained in a Dulbecco's modified Eagle's medium/nutrient mixture Ham's F-12 (Sigma-Aldrich) supplemented with 5% tetracycline-screened fetal bovine serum (Sigma-Aldrich), 15 mM HEPES, 500 μg/mL G418, 100 U/mL of penicillin G sodium, 100 μg/mL streptomycin, 29.2 mg/mL L-glutamine, 100 μg/mL Zeocin, and 5 μg/mL Blasticidin. Media components were, unless otherwise noted, purchased from Fisher Scientific. Twenty-four hours before recordings, spent media was aspirated and replaced with fresh media that lacked antibiotics. Expression was induced with the addition of doxycycline at a final concentration of 1 μg/mL.

For IonWorks Barracuda (IWB) experiments, cells were cultured in Corning T-150 flasks (Corning, NY) to a confluence of 85%–95%. Cells were washed once with Dulbecco's phosphate-buffered saline without calcium and magnesium and then dissociated by incubating in 3 mL of 0.25% Trypsin for 8 min at 37°C. Cells were resuspended in 9 mL fresh media, gently triturated, and centrifuged for 4 min at 1,000 rpm. The supernatant was aspirated, and cells were resuspended in external solution (see "Solutions" section) to a final concentration of 2.5–3.5M cells/mL.

Solutions

Chemicals used in solution preparations were, unless otherwise noted, purchased from Sigma-Aldrich. External solution composition was 140 mM NaCl, 5 mM KCl (Teknova, Hollister, CA), 2 mM $CaCl_2$, 1 mM $MgCl_2$, 10 mM HEPES, and 10 mM Glucose, pH adjusted to 7.4 with NaOH. Internal solution composition was 90 mM K-gluconate, 40 mM KCl, 3.2 mM EGTA, 3.2 mM $MgCl_2$, and 5 mM HEPES, pH adjusted to 7.25 with KOH. The membrane perforating agent amphotericin B was prepared daily as a 27 mg/mL stock solution in DMSO and then added to the internal solution to a final concentration of 0.1 mg/mL. All final test and control solutions contained 0.1% DMSO. Test article dilutions were prepared in 384-well plates and diluted using an acoustic dispensing platform (Labcyte Echo, San Jose, CA).

Electrophysiological Recordings

Resuspended cells were placed on the IWB system, external solution was added to a 384-well patch plate, and a hole test was performed to identify wells with blocked holes and determine offset voltages. Cells were then mixed and added to the patch plate (9 μL/well). Two seal tests were performed; internal solution with perforating agent was exchanged, allowing ~8 min to obtain access before a third seal test was performed. All recordings used the population patch clamp (PPC) mode with a sampling frequency of 1 kHz. The command voltage protocol consisted of a family of 1s voltage steps applied every 5.5 s from a holding potential of −80 mV and ranging from −80 to +40 mV. Following a baseline recording, test compounds were added, allowed to equilibrate for 6 min, and effects were assessed (see "Data Analysis" section) with an identical command voltage protocol. Unlike previous platform design iterations, the IWB does not suffer from discontinuous voltage clamp during liquid additions. For a detailed assay protocol, see *Table 1*.

Data Analysis

Data acquisition, leak subtraction, and metrics exports were performed using IWB software (Molecular Devices Corporation, Union City, CA). Leak currents were defined as currents activated during a prepulse from −100 to −80 mV and were digitally subtracted from each data point. For each well, current amplitudes during the last 10 ms of each voltage step were averaged and exported. Current amplitude measurements were converted to conductance (G) by the following formula: $G = I/(V - E_K)$, where I = current, V = step potential, and E_K = reversal potential for potassium (−84 mV). E_K was calculated based on the composition of the internal and external recording solutions. Conductance values after compound addition were normalized to the precompound maximal conductance (conductance at +40 mV) for the same well. Using Microsoft Excel (Microsoft Corporation, Redmond, WA) and XLFit (ID Business Solutions Limited, Guildford, United Kingdom), conductance-voltage (G-V) curves were generated and fit to the Boltzmann equation $y = \text{Bottom} + (\text{Top-Bottom})/(1 + \text{EXP}(V_m - V_{0.5}/k))$.

Unless otherwise noted, data are presented as average ± standard deviation (SD).

RESULTS/DISCUSSION

IWB Assay Performance

In an effort to find and characterize modulators of Kv7 channels, assays were developed on the IWB automated electrophysiology platform using HEK293 cells expressing either heteromeric Kv7.2/7.3 or Kv7.3/7.5 channels. The PPC

Table 1. IonWorks Barracuda Kv7 Electrophysiology Protocol

Step	Parameter	Value	Description
1	Prime patch plate	11 μL	External solution
2	Hole test	−10 mV, 60 ms	Step from 0 mV
3	Wash patch plate	20 μL, 5 μL/s	External solution
4	Prime patch plate	11 μL	External solution
5	Add cells	9 μL	~27,000 cells/well
6	Test seal-1	−80 mV, 60 ms	Step from holding at −70 mV
7	Form seal	120 s	Wait
8	Test seal-2	−80 mV, 60 ms	Step from holding at −70 mV
9	Establish access	Amphotericin B 0.1 mg/mL	Perfuse 115 s, incubate 240 s
10	Test seal-3	−80 mV, 60 ms	Step from holding at −70 mV
11	Set Vhold (rest)	Vhold = −80 mV	
12	I–V family-baseline	−80 to +40 mV (1 s, 10 mV steps)	Sweep to sweep = 5500 ms
13	Add test compound	10 μL, 2 μL/s	Incubate 6 min
14	I–V family-post compound	−80 to +40 mV (1 s, 10 mV steps)	Sweep to sweep = 5500 ms
15	Wash e-plate	2 × 0.5 min	0.9% NaCl; sonication; discard tips

mode of the IWB instrument was used to record ensemble currents from up to 64 cells per well.[45] In this mode, Kv7.2/7.3 cells were sealed well with success rates of 99% and typical seal resistances of 28–170 MΩ. Similarly, Kv7.3/Kv7.5 cells were sealed with success rates of 98% and typical seal resistances of 20–114 MΩ. *Figure 1A* shows a family of Kv7.2/7.3 current traces elicited by 1s voltage steps to voltages ranging from −80 to +40 mV. Currents display the relatively slow activation and deactivation rates characteristic for Kv7 channels, and current amplitudes (at +40 mV) were 3.1 ± 0.2 nA. Software filters were utilized to remove any wells that displayed current amplitudes <1 nA (at +40 mV). Average currents at the end of each voltage step were converted to conductance values, normalized and plotted as a function of voltage, as illustrated in the panel on the right. Fitting Boltzmann curves to the data yielded an average half activation voltage of −4.4 ± 0.1 mV, in good agreement with values of −11.3 ± 1.6 mV on the Q-patch platform.[41] Similarly, *Figure 1B* shows 1s current traces for Kv7.3/7.5 heteromeric channels. Wells with current amplitudes <0.8 nA were removed from the analysis. Remaining current amplitudes for this cell line were 1.6 ± 0.3 nA at +40 mV. A Boltzmann fit to the normalized conductance curves yielded an average half activation voltage of −17.6 ± 0.1 mV, similar to the half activation voltage of −34.8 ± 1.6 mV published for Kv7.3/7.5 currents expressed in CHO cells.[46]

To assess the stability of maximal conductance and voltage of half-activation of Kv7.2/7.3 currents over the time period of the assay, these parameters were compared before and after a 6 min incubation with a range of DMSO concentrations in assay buffer. DMSO concentrations ≥0.09% caused a concentration dependent decrease in the maximal conductance (G_{max}), normalized to pre-DMSO controls (*Fig. 2A*), whereas the voltage of half activation was not affected by DMSO concentrations ≤0.75% (*Fig. 2B*). Based on these results and the need to evaluate test compounds available as 10 mM DMSO stock solutions, 0.1% DMSO was chosen for use in the assay. After a 6 min incubation with 0.1% DMSO in assay buffer, G_{max}, normalized to baseline values, was 1.05 ± 0.05 (n = 30) and 0.89 ± 0.05 (n = 30) for Kv7.2/7.3 and Kv7.3/7.5 currents, respectively; voltages of half activation were not changed.

Kv7 Pharmacology

A set of known Kv7 modulators was tested for effects on G_{max} and $V_{0.5}$ to further validate the IWB Kv7.2/7.3 and Kv7.3/7.5 assays. ML252 has been identified as a potent and selective inhibitor of Kv7 channels other than Kv7.1.[47] In the IWB assay, ML252 inhibited Kv7.2/7.3 currents in a concentration dependent manner without effects on the voltage range of activation (*Fig. 2C)*. Plotting G_{max} as a function of concentration and fitting a 4-parameter logistic equation to the data yielded an IC_{50} of 0.29 μM (geometric mean) with a SEM of 0.08 and a slope of 1.3 ± 0.5 (n = 6); comparable to the IC_{50} of 0.12 μM obtained in an IonWorks Quattro assay.[47] Kv7.3/7.5 currents were inhibited by ML252 in a similar manner (*Fig. 2D)* with an IC_{50} of 0.23 μM (SEM 0.05) and a slope of 1.3 ± 0.5 (n = 6). At saturating concentrations, ML252 inhibited 90% ± 4% and 82% ± 4% of the Kv7.2/7.3 and Kv7.3/7.5 currents, respectively, demonstrating that the majority of the current activated during voltage steps to +40 mV was conducted by Kv7 channels.

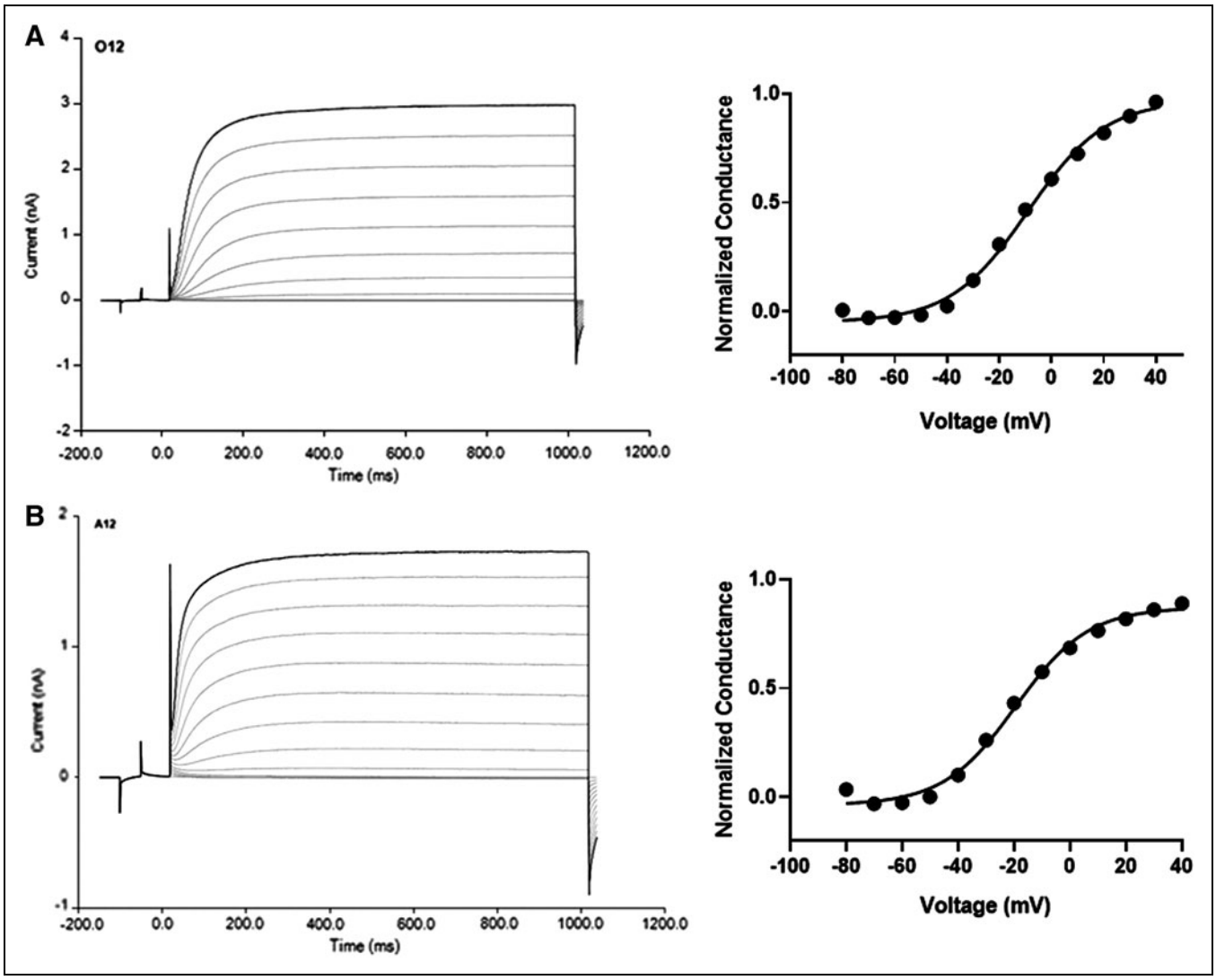

Fig. 1. Kv7.2/7.3 **(A)** and Kv7.3/7.5 **(B)** currents recorded on IWB. *Left panels* illustrate IWB current traces activated by steps from −80 to +40 mV in 10 mV increments. *Right hand panels* show the normalized conductance-voltage curves for the exemplar traces. IWB, IonWorks Barracuda.

Flupirtine and its close analog retigabine are well-known activators of Kv7.2–7.5 channels.[48] In the IWB assay, flupirtine induced a concentration-dependent shift of the voltage dependence ($\Delta V_{0.5}$) of Kv7.2/7.3 current activation to more hyperpolarized (negative) voltages (*Fig. 3A*, left panel). In addition, flupirtine caused a small but significant increase in G_{max}. There was no change in the slope of the conductance curves in the presence of flupirtine and no evidence of biphasic curves reported by Yau *et al*. in the oocyte expression system.[24] Fitting a 4-parameter logistic equation to the concentration dependence of $V_{0.5}$ for 10 representative experiments yielded an EC_{50} of 4.03 μM (geometric mean) with SEM 0.42 and a slope of 1.4 ± 0.4. The change in G_{max} was too small to be analyzed reliably. Since it was readily available and not subject to restrictions, flupirtine was chosen as a reference standard to monitor the uniformity and stability of the assay over time. The middle and right panels in *Figure 3A* illustrate the stability of $\Delta V_{0.5}$ and G_{max} in the presence of 10 μM flupirtine across 431 determinations spanning a >2-year period. The average $\Delta V_{0.5}$ was −23.9 ± 4.0 mV (mean ± SD) with lower to upper 95% confidence intervals (CIs) of −23.5 to −24.3 mV, respectively. The average normalized G_{max} was 1.18 ± 0.08 with lower and upper 95% CIs of 1.17–1.19, respectively.

Flupirtine was also a potent activator of recombinant Kv7.3/7.5 currents (*Fig. 3B*), shifting the voltage dependence of activation and increasing G_{max}. Interestingly, the $\Delta V_{0.5}$

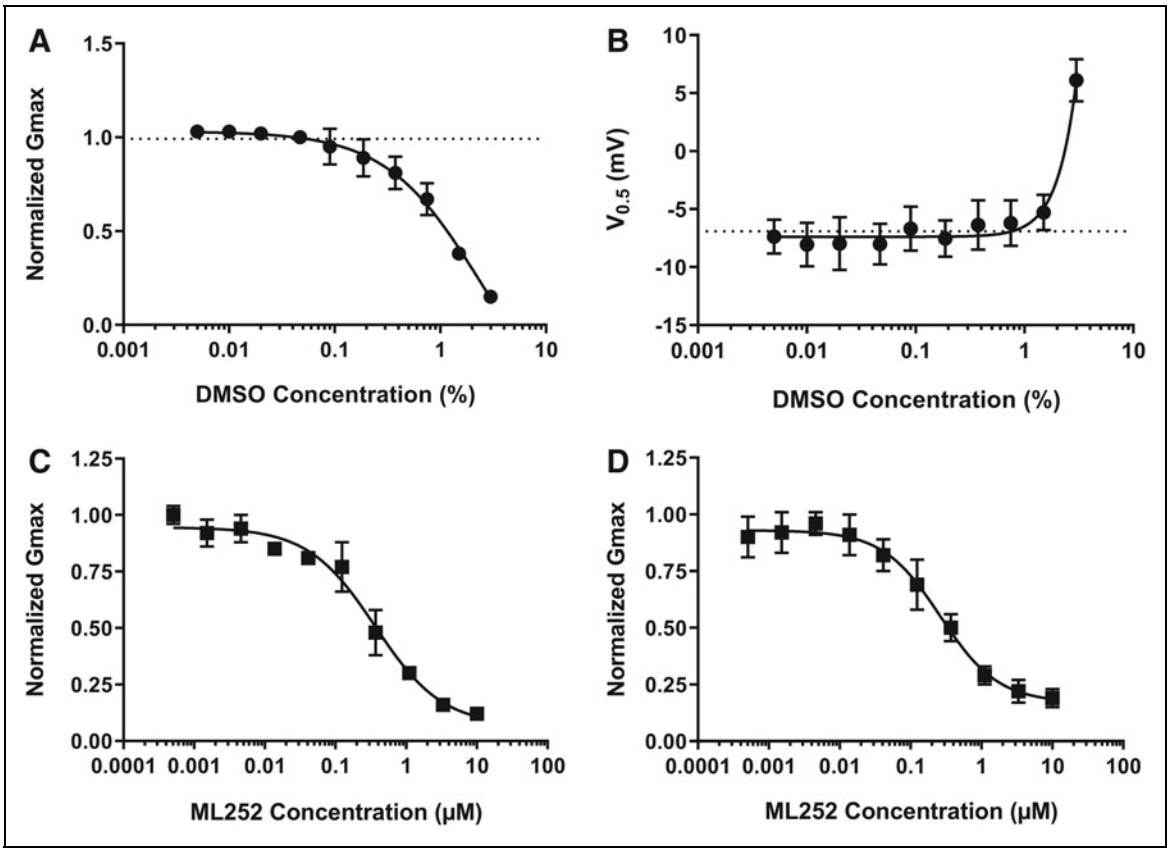

Fig. 2. DMSO tolerance and inhibition by the Kv7 selective compound ML252. DMSO tolerance was investigated by plotting normalized conductance at +40 mV **(A)** and voltage of half activation ($V_{0.5}$) **(B)** as a function of DMSO concentration ($n=15$). *Dotted lines* are representative of buffer controls (external solution without DMSO). **(C, D)** The Kv7 selective inhibitor ML252 reduced the maximal conductance of Kv7.2/7.3 **(C)** and Kv7.3/7.5 **(D)** currents in a concentration dependent manner. DMSO, dimethyl sulfoxide.

caused by 10 μM flupirtine (−18.3 ± 3.9 mV, $n=382$) was smaller than that for Kv7.2/7.3, while the increase in G_{max} (1.65 ± 0.18, $n=382$) was larger ($p<0.05$). Attempts at fitting a logistic equation to the $V_{0.5}$ data for Kv7.3/7.5 typically resulted in curves that did not plateau, suggesting that the potency may be somewhat lower than what was observed for Kv7.2/7.3. In contrast, the larger increase in G_{max} seen with Kv7.3/7.5 allowed for a reliable analysis of the concentration dependence, yielding an EC_{50} of 3.12 μM (geometric mean) with SEM 0.72 and a slope of 1.2 ± 0.5 ($n=9$). Beyond the scope of this article, the molecular mechanisms underlying this difference between the two Kv7 subtypes would be an interesting topic of investigation. In this regard, it is interesting to note that retigabine caused a larger increase in G_{max} in Kv7.3 homomeric channels than in Kv7.2 or in heteromeric Kv7.2/7.3 channels.[49,50] Unfortunately, channels, including Kv7.5 subunits, were not tested in this study. In addition, point mutations in the pore region of Kv7.3 had differential effects on the voltage shift and the change in G_{max} induced by retigabine.[21]

To further investigate the utility of the IWB assay, two compounds representing scaffolds distinct from flupirtine were tested. Similar to results with flupirtine, benzothiazolone hydrazone from a 2010 report by Fritch *et al.*[44] produced concentration dependent effects on the conductance-voltage curves for Kv7.2/7.3 (*Fig. 4A*) and Kv7.3/7.5 (*Fig. 4B*), affecting both $V_{0.5}$ and G_{max}. Data for each of these parameters were plotted as a function of benzothiazolone hydrazone concentration and fit with a 4-parameter logistic equation. *Figure 4C* shows the simultaneous fit of all $V_{0.5}$ values. For Kv7.2/7.3 channels, $V_{0.5}$ was left-shifted with an EC_{50} of 1.7 μM, a slope of 1.1, and a maximal effect of −52 mV. Benzothiazolone hydrazone shifted the $V_{0.5}$ of Kv7.3/7.5 channels with an EC_{50} of 1.2 μM, a slope of 1.0, and a maximal effect of −57 mV. Comparing the effects on the two channel subtypes, neither the EC_{50} nor the maximal effect was significantly different ($p=0.67$ and 0.64, respectively). G_{max} for both channels was increased in the presence of benzothiazolone hydrazone with an EC_{50} of 0.5 μM, a slope of 1.8, and a maximal effect of 1.3 for Kv7.2/7.3 channels and an EC_{50} of

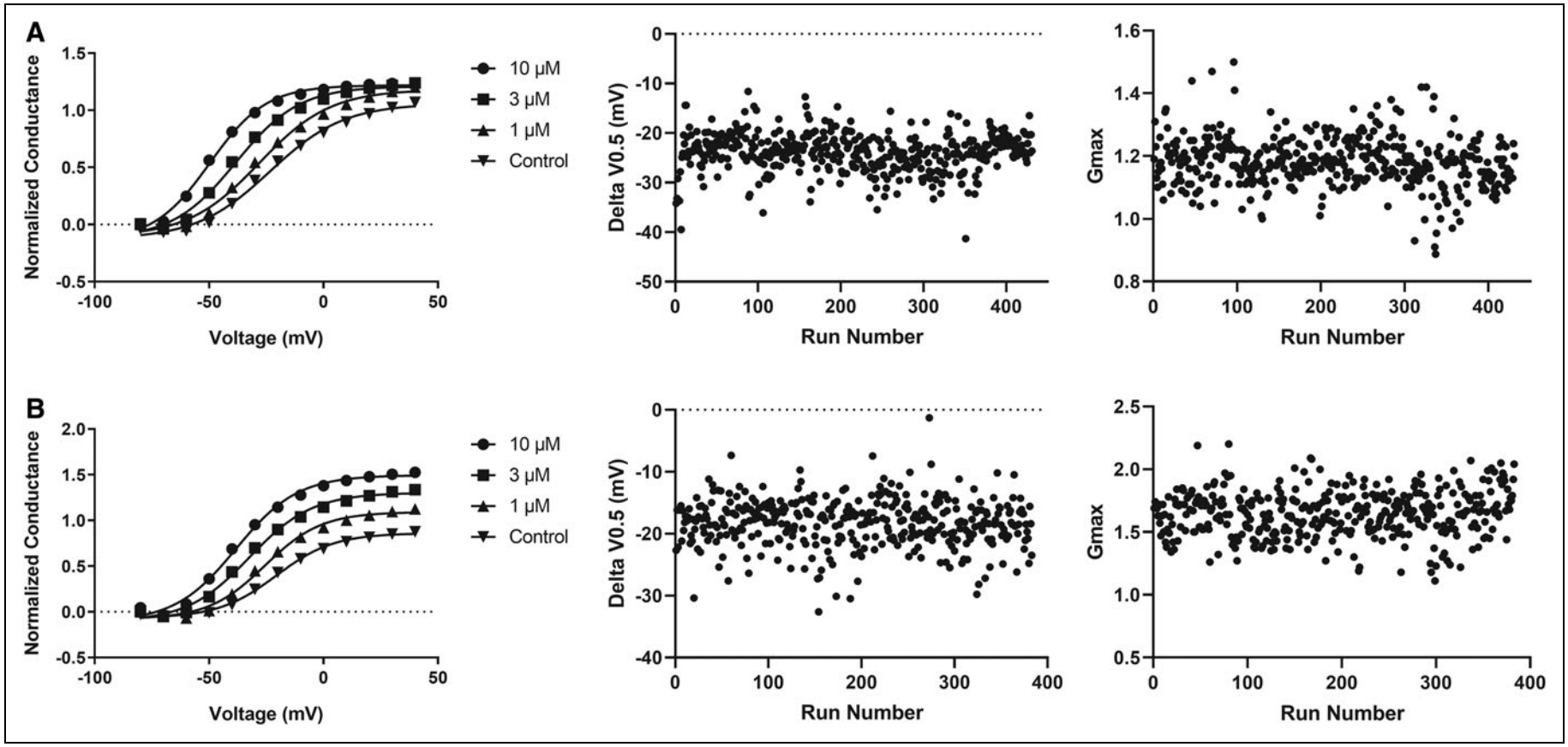

Fig. 3. Activation by flupirtine and assay performance for Kv7.2/7.3 **(A)** and Kv7.3/7.5 **(B)**. *Left panels* show overlays of normalized conductance-voltage curves for representative wells receiving either buffer control (*black down-pointing triangle*) or 1 μM (*black up-pointing triangle*), 3 μM (*black square*), or 10 μM (*black circle*) flupirtine. Control charting showing the $\Delta V_{0.5}$ (*middle*) and relative G_{max} (*right*) derived from conductance-voltage curves in the presence of 10 μM flupirtine for 431 (**A**; Kv7.2/7.3) and 382 (**B**; Kv7.3/7.5) determinations conducted over >2 years as a function of run number.

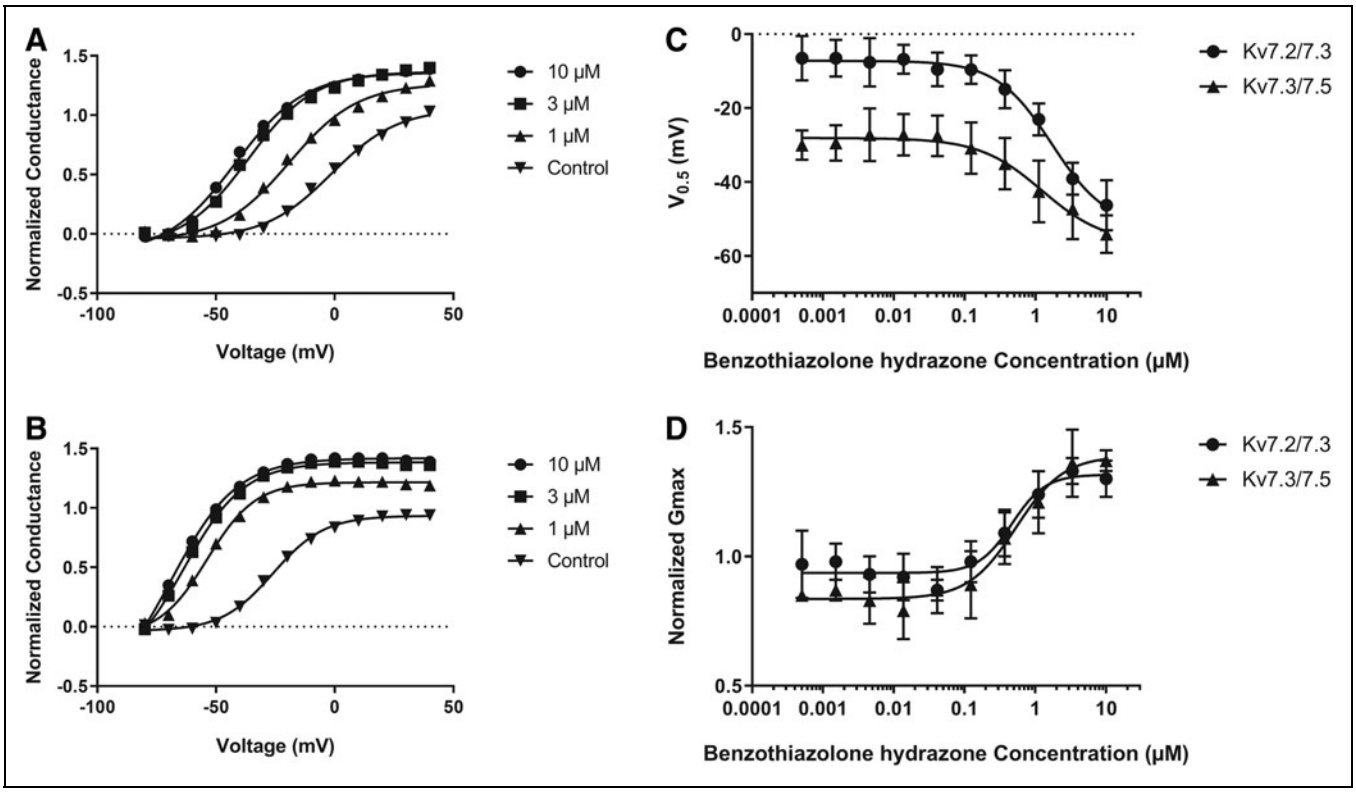

Fig. 4. Activation of Kv7.2/7.3 **(A)** and Kv7.3/7.5 **(B)** by benzothiazolone hydrazone. *Left hand panels* show an overlay of normalized conductance-voltage curves for representative wells receiving either buffer control (*black down-pointing triangle*) or 1 μM (*black up-pointing triangle*), 3 μM (*black square*), or 10 μM (*black circle*) benzothiazolone hydrazone. **(C)** Concentration dependence of the hyperpolarizing shifts in $V_{0.5}$ for Kv7.2/7.3 (*black circle*) and Kv7.3/7.5 (*black up-pointing triangle*) in the presence of benzothiazolone hydrazone. **(D)** Concentration dependence of G_{max} for Kv7.2/7.3 (*black circle*) and Kv7.3/7.5 (*black up-pointing triangle*) in the presence of benzothiazolone hydrazone.

0.5 μM, a slope of 1.3, and a maximal effect of 1.4 for Kv7.3/7.5 (*Fig. 4D*). EC_{50}s and maximal effect were not different between the two channel subtypes ($p = 0.70$ and 0.21, respectively). The potency of Kv7.2/7.3 modulation was significantly lower than the EC_{50} of 50 nM from a $^{86}Rb^{+}$ efflux assay reported in the original publication.[44] However, there is precedence for significant differences between potencies measured for the same compounds in flux and electrophysiology assays (see, *e.g.*, Yue *et al.*[42]), and the publication on benzothiazolone hydrazine did not include any known reference compounds to assess the sensitivity and dynamic range of the efflux assay.

ICA-27243 was reported to be a selective potentiator of Kv7.2/7.3 channels.[32,51] In agreement with the expectation, 1 μM ICA-27243 clearly shifted the voltage dependence of Kv7.2/7.3 channel activation to more hyperpolarized voltages (*Fig. 5A*) but had no effect on the conductance-voltage relationship of Kv7.3/7.5 channels (*Fig. 5B*). At 10 μM, ICA-27243 increased G_{max} of Kv7.3/7.5, an effect that was not seen at lower concentrations.

Comparing the concentration dependence of the $V_{0.5}$ (*Fig. 5C*) and G_{max} (*Fig. 5D*) for the two channel subtypes illustrates the selectivity of ICA-27243. Kv7.2/7.3 currents showed a clear concentration dependent increase in the absolute $V_{0.5}$ with an EC_{50} of 3.1 μM, a slope of 0.9, and a maximal effect of −42 mV. These data agree well with published values of an EC_{50} of 4.8 μM and a slope of 0.8.[32] In contrast to Kv7.2/7.3 and in agreement with published data,[30,32] $V_{0.5}$ values for Kv7.3/7.5 were not different from DMSO controls at any concentration tested ($p = 0.34$ at 10 μM). The effect of ICA-27243 on the G_{max} of Kv7.2/7.3, although small, was concentration dependent and reached significance at 1.1 and 3.3 μM. Fitting the data with a 4-parameter logistic equation indicated an EC_{50} of 0.23 μM and a maximal effect of 1.12. Excluding the data at 10 μM only slightly changed the results (EC_{50} of 0.32 μM, maximal effect of 1.16). ICA-27243 also increased the G_{max} of Kv7.3/7.5 currents. The increase was significant at 3.3 and 10 μM but did not saturate. The difference in the concentration dependence of the effects on $V_{0.5}$ and G_{max}, seen with both channel

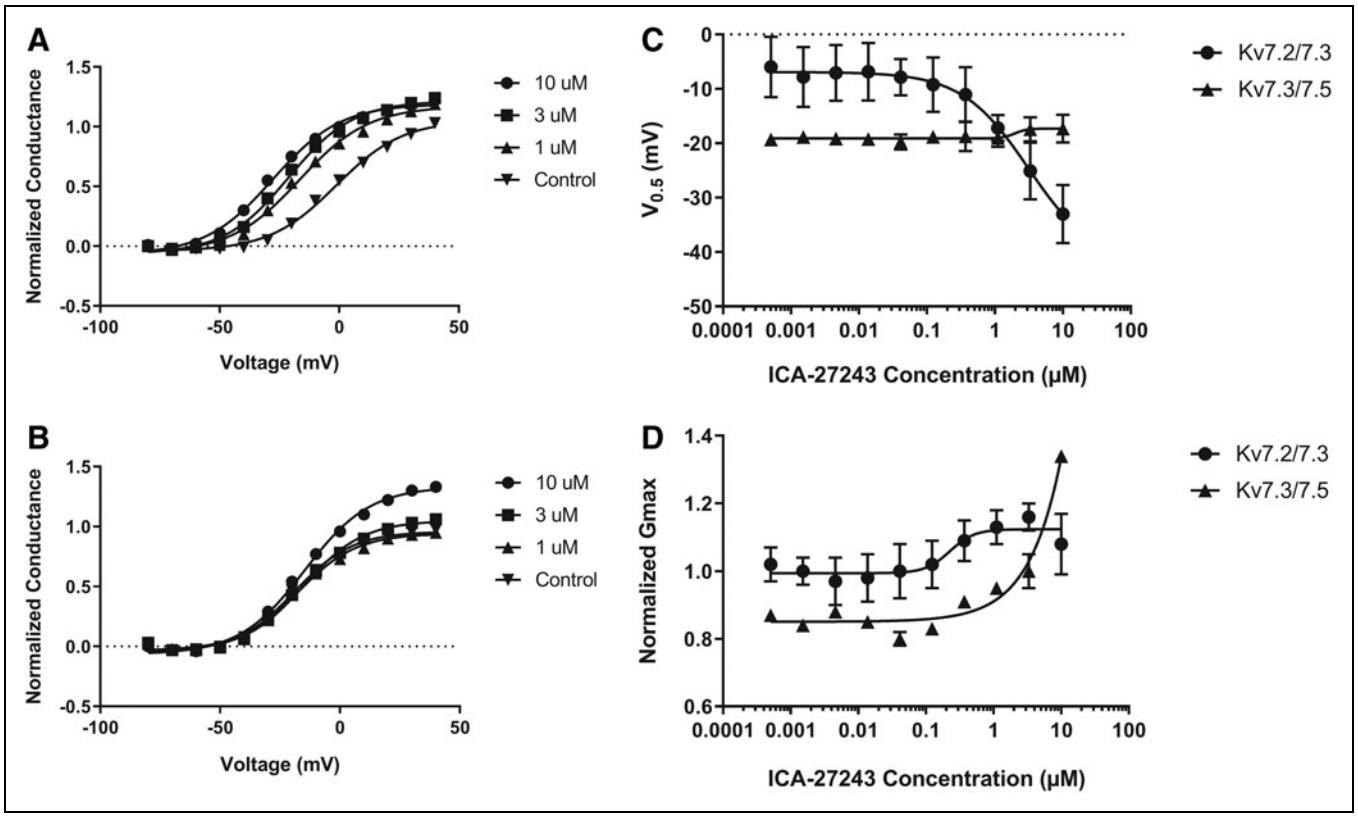

Fig. 5. Activation of Kv7.2/7.3 **(A)** and Kv7.3/7.5 **(B)** by ICA-27243. *Left hand panels* show an overlay of normalized conductance-voltage curves for representative wells receiving either buffer control (*black down-pointing triangle*) or 1 μM (*black up-pointing triangle*), 3 μM (*black square*), or 10 μM (*black circle*) ICA-27243. **(C)** Concentration dependence of the hyperpolarizing shifts in $V_{0.5}$ for Kv7.2/7.3 (*black circle*) and Kv7.3/7.5 (*black up-pointing triangle*) in the presence of ICA-27243. **(D)** Concentration dependence of G_{max} for Kv7.2/7.3 (*black circle*) and Kv7.3/7.5 (*black up-pointing triangle*) in the presence of ICA-27243.

subtypes, suggests that ICA-27243 may be interacting with more than one binding site. Studies on chimeric constructs show that effects of ICA-27243 on the voltage dependence of channel activation are mediated by interactions with the voltage sensor domain.[30] Intriguingly, mutagenesis studies with the closely related molecule ICA-069672 identified an alanine-to-proline point mutation in transmembrane segment S3 of Kv7.2 that nearly eliminated the effects on $V_{0.5}$ but retained effects on G_{max}, also suggesting different molecular determinants for the two effects.[31]

Assigning Potency Values

Efficiently prioritizing compounds for drug discovery requires a measure of potency that is relevant to the desired mechanism of action. Throughout the nervous system, excitability is largely controlled by resting membrane potential, in concert with the complement of ion channels expressed in a given cell type. In small diameter DRG neurons, modulating the activity of Kv7 channels had the greatest influence on resting membrane potential, when comparing modulators of various ion channel subtypes known to be expressed in DRG neurons.[4] This finding suggests that potency of a test compound should reflect its effects on channel conductance near the resting membrane potential. The resting membrane potential of DRG neurons at the soma was reported as –60 mV,[4] corresponding to the foot of the activation curve of Kv7.2/7.3 channels. Current amplitudes at these hyperpolarized voltages are affected by changes in both $V_{0.5}$ and G_{max}. Therefore, fitting compound mediated effects on the conductance at a fixed voltage near the foot of the activation curve may generate EC_{50}s that can be used to compare and rank order compound potencies.

The voltage dependence of channel activation differs among Kv7 channel subtypes. Therefore, it may be beneficial to base voltages used for potency analysis on fractional current activation rather than using a fixed voltage. Using the voltage at which the conductance reaches 15% of the maximal conductance under control conditions, hereafter referred to as $V_{0.15}$, represents a compromise between choosing a voltage near the DRG resting membrane potential and the ability to accurately

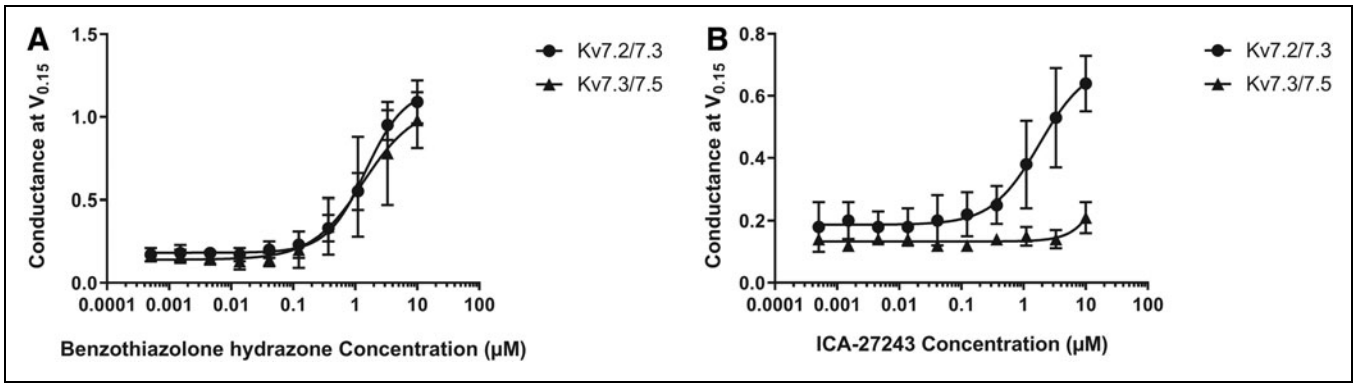

Fig. 6. Kv7 current increases near the activation threshold. **(A)** Concentration dependence of the conductance at voltages (Vo.15) corresponding to 15% current activation under control conditions for Kv7.2/7.3 (*black circle*) and Kv7.3/7.5 (*black up-pointing triangle*) in the presence of benzothiazolone hydrazone. **(B)** Concentration dependence of the conductance at Vo.15 for Kv7.2/7.3 (*black circle*) and Kv7.3/7.5 (*black up-pointing triangle*) in the presence of ICA-27243.

determine the corresponding conductance. *Figure 6A* and *B* shows the concentration dependence of the conductance at the $V_{0.15}$ for benzothiazolone hydrazone and ICA-27243, respectively. Conductance values ($G_{0.15}$) were normalized to the maximal conductance before compound addition.

As expected, the concentration–response curves describing the effects of benzothiazolone hydrazone on the $G_{0.15}$ are similar for Kv7.2/7.3 and Kv7.3/7.5 channels. Fitting a traditional 4-parameter logistic equation to the data yielded EC_{50}s of 1.49 and 1.35 μM for Kv7.2/7.3 and Kv7.3/7.5, respectively ($p=0.86$). Concentration response curves for the effects of ICA-27243 on the $G_{0.15}$ clearly show the activation of Kv7.2/7.3 with an EC_{50} of 1.82 μM. For Kv7.3/7.5, while there was a trend for higher $G_{0.15}$ values in the presence of 10 μM ICA-27243, the increase did not reach statistical significance over baseline ($p=0.43$), demonstrating the selectivity of this compound.

Many test compounds produced effects on $G_{0.15}$ that did not reach saturation, resulting in an undetermined EC_{50}. Relatively weak affinity and limited solubility may both be contributors to this observation. An analysis that returns a potency value for such compounds is desirable and requires a parameter that is not relative to the complete concentration–response curve. Consequently, we defined the potency measure as the concentration that increased the conductance at $V_{0.15}$ by a fixed multiple. Targeting a doubling of the conductance returned reproducible results for the vast majority of test compounds. Therefore, we chose the EC_{200} as a potency measure and defined it as the concentration of test compound that increased the conductance at $V_{0.15}$ from 15% to 30% of the G_{max} in vehicle controls. EC_{200} values were obtained from the least squares fit of concentration–response curves such as those shown in *Figure 6*. Results were reproducible as illustrated by the standard errors and are presented in *Table 2*.

The EC_{200} may offer an advantage for predicting relative effects on neuronal excitability, if compounds vary significantly in their efficacy, that is, the maximum achievable conductance increase. Membrane excitability, in terms of action potential generation, is essentially a threshold effect, dependent on the amplitude and voltage dependence of depolarizing currents coupled with the membrane resistance. Consequently, the hyperpolarizing current required to oppose action potential generation should also be based on a threshold. This hypothesis is supported by studies comparing several Kv7 potentiators with regard to their ability to restore threshold M current amplitudes in DRG neurons after PIP_2 depletion.[36] Despite differential effects on $V_{0.5}$ and G_{max}, all four compounds studied restored current amplitudes to their control levels. Preliminary data suggest that the EC_{200} values correlate well with the ability of compounds to inhibit neuronal excitability *in vitro* (article in preparation). However, the

Table 2. Potency of Kv7 Activators

	Kv7.2/7.3 EC200			Kv7.3/7.5 EC200		
	Geo mean (μM)	SEM	*n*	Geo Mean (μM)	SEM	*n*
Flupirtine	2	0.05	431	1.58	0.05	384
Benzothiazolone hydrazone	0.48	0.08	6	0.79	0.39	4
ICA-27243	1.15	0.28	7	>10	NA	2

SEM, standard error of the mean.

usefulness of the EC_{200} will ultimately be determined by how well it correlates with the concentration dependence of pharmacodynamics effects, either in *in vivo* pain models or potentially in tissue-based surrogates.

DISCLOSURE STATEMENT

The authors are all employees of Eli Lilly and Company and declare no conflicts of interest.

FUNDING INFORMATION

No funding was received for this article.

REFERENCES

1. Goldberg DS, McGee SJ: Pain as a global public health priority. *BMC Public Health* 2011;11:770.
2. Walker G: The opioid crisis: a 21st century pain. *Drugs Today (Barc)* 2018;54: 283–286.
3. Wickenden AD, McNaughton-Smith G: Kv7 channels as targets for the treatment of pain. *Curr Pharm Des* 2009;15:1773–1798.
4. Du X, Hao H, Gigout S, *et al.*: Control of somatic membrane potential in nociceptive neurons and its implications for peripheral nociceptive transmission. *Pain* 2014;155:2306–2322.
5. Huang H, Trussell LO: KCNQ5 channels control resting properties and release probability of a synapse. *Nat Neurosci* 2011;14:840–847.
6. Suh BC, Hille B: Recovery from muscarinic modulation of M current channels requires phosphatidylinositol 4,5-bisphosphate synthesis. *Neuron* 2002;35: 507–520.
7. Brown DA, Adams PR: Muscarinic suppression of a novel voltage-sensitive K+ current in a vertebrate neurone. *Nature* 1980;283:673–676.
8. Adams PR, Brown DA, Constanti A: Pharmacological inhibition of the M-current. *J Physiol* 1982;332:223–262.
9. Bal M, Zhang J, Zaika O, Hernandez CC, Shapiro MS: Homomeric and heteromeric assembly of KCNQ (Kv7) K+ channels assayed by total internal reflection fluorescence/fluorescence resonance energy transfer and patch clamp analysis. *J Biol Chem* 2008;283:30668–30676.
10. Blackburn-Munro G, Dalby-Brown W, Mirza NR, Mikkelsen JD, Blackburn-Munro RE: Retigabine: chemical synthesis to clinical application. *CNS Drug Rev* 2005;11:1–20.
11. Liang GH, Jin Z, Ulfendahl M, Jarlebark L: Molecular analyses of KCNQ1-5 potassium channel mRNAs in rat and guinea pig inner ears: expression, cloning, and alternative splicing. *Acta Otolaryngol* 2006;126:346–352.
12. Kanaumi T, Takashima S, Iwasaki H, Itoh M, Mitsudome A, Hirose S: Developmental changes in KCNQ2 and KCNQ3 expression in human brain: possible contribution to the age-dependent etiology of benign familial neonatal convulsions. *Brain Dev* 2008;30:362–369.
13. Geiger J, Weber YG, Landwehrmeyer B, Sommer C, Lerche H: Immunohistochemical analysis of KCNQ3 potassium channels in mouse brain. *Neurosci Lett* 2006;400: 101–104.
14. Passmore GM, Selyanko AA, Mistry M, *et al.*: KCNQ/M currents in sensory neurons: significance for pain therapy. *J Neurosci* 2003;23:7227–7236.
15. Schroeder BC, Hechenberger M, Weinreich F, Kubisch C, Jentsch TJ: KCNQ5, a novel potassium channel broadly expressed in brain, mediates M-type currents. *J Biol Chem* 2000;275:24089–24095.
16. Kumar M, Reed N, Liu R, Aizenman E, Wipf P, Tzounopoulos T: Synthesis and evaluation of potent KCNQ2/3-specific channel activators. *Mol Pharmacol* 2016;89:667–677.
17. Devulder J: Flupirtine in pain management: pharmacological properties and clinical use. *CNS Drugs* 2010;24:867–881.
18. Jankovic S, Ilickovic I: The preclinical discovery and development of ezogabine for the treatment of epilepsy. *Expert Opin Drug Discov* 2013;8:1429–1437.
19. Schenzer A, Friedrich T, Pusch M, *et al.*: Molecular determinants of KCNQ (Kv7) K+ channel sensitivity to the anticonvulsant retigabine. *J Neurosci* 2005;25: 5051–5060.
20. Wuttke TV, Seebohm G, Bail S, Maljevic S, Lerche H: The new anticonvulsant retigabine favors voltage-dependent opening of the Kv7.2 (KCNQ2) channel by binding to its activation gate. *Mol Pharmacol* 2005;67:1009–1017.
21. Lange W, Geissendorfer J, Schenzer A, *et al.*: Refinement of the binding site and mode of action of the anticonvulsant Retigabine on KCNQ K+ channels. *Mol Pharmacol* 2009;75:272–280.
22. Syeda R, Santos JS, Montal M: The sensorless pore module of voltage-gated K+ channel family 7 embodies the target site for the anticonvulsant retigabine. *J Biol Chem* 2016;291:2931–2937.
23. Kim RY, Yau MC, Galpin JD, *et al.*: Atomic basis for therapeutic activation of neuronal potassium channels. *Nat Commun* 2015;6:8116.
24. Yau MC, Kim RY, Wang CK, *et al.*: One drug-sensitive subunit is sufficient for a near-maximal retigabine effect in KCNQ channels. *J Gen Physiol* 2018;150: 1421–1431.
25. Wickenden AD, Yu W, Zou A, Jegla T, Wagoner PK: Retigabine, a novel anti-convulsant, enhances activation of KCNQ2/Q3 potassium channels. *Mol Pharmacol* 2000;58:591–600.
26. Dalby-Brown W, Jessen C, Hougaard C, *et al.*: Characterization of a novel high-potency positive modulator of K(v)7 channels. *Eur J Pharmacol* 2013;709: 52–63.
27. Manville RW, Papanikolaou M, Abbott GW: Direct neurotransmitter activation of voltage-gated potassium channels. *Nat Commun* 2018;9:1847.
28. Manville RW, Abbott GW: Gabapentin is a potent activator of KCNQ3 and KCNQ5 potassium channels. *Mol Pharmacol* 2018;94:1155–1163.
29. Zhang F, Liu Y, Tang F, *et al.*: Electrophysiological and pharmacological characterization of a novel and potent neuronal Kv7 channel opener SCR2682 for antiepilepsy. *FASEB J* 2019;33:9154–9166.
30. Padilla K, Wickenden AD, Gerlach AC, McCormack K: The KCNQ2/3 selective channel opener ICA-27243 binds to a novel voltage-sensor domain site. *Neurosci Lett* 2009;465:138–142.
31. Wang AW, Yang R, Kurata HT: Sequence determinants of subtype-specific actions of KCNQ channel openers. *J Physiol* 2017;595:663–676.
32. Wickenden AD, Krajewski JL, London B, *et al.*: N-(6-chloro-pyridin-3-yl)-3,4-difluoro-benzamide (ICA-27243): a novel, selective KCNQ2/Q3 potassium channel activator. *Mol Pharmacol* 2008;73:977–986.
33. Wang AW, Yau MC, Wang CK, *et al.*: Four drug-sensitive subunits are required for maximal effect of a voltage sensor-targeted KCNQ opener. *J Gen Physiol* 2018;150:1432–1443.
34. Yu H, Wu M, Townsend SD, *et al.*: Discovery, synthesis, and structure activity relationship of a series of N-aryl- bicyclo[2.2.1]heptane-2-carboxamides: Characterization of ML213 as a novel KCNQ2 and KCNQ4 potassium channel opener. *ACS Chem Neurosci* 2011;2:572–577.
35. Blom SM, Rottlander M, Kehler J, Bundgaard C, Schmitt N, Jensen HS: From pan-reactive KV7 channel opener to subtype selective opener/inhibitor by addition of a methyl group. *PLoS One* 2014;9:e100209.
36. Linley JE, Pettinger L, Huang D, Gamper N: M channel enhancers and physiological M channel block. *J Physiol* 2012;590:793–807.
37. Hamill OP, Marty A, Neher E, Sakmann B, Sigworth FJ: Improved patch-clamp techniques for high-resolution current recording from cells and cell-free membrane patches. *Pflugers Arch* 1981;391:85–100.
38. Yang S, Lu D, Ouyang P: Design, synthesis and evaluation of substituted piperidine based KCNQ openers as novel antiepileptic agents. *Bioorg Med Chem Lett* 2018;28:1731–1735.
39. Wang K, McIlvain B, Tseng E, *et al.*: Validation of an atomic absorption rubidium ion efflux assay for KCNQ/M-channels using the ion Channel Reader 8000. *Assay Drug Dev Technol* 2004;2:525–534.

40. Beacham DW, Blackmer T, M OG, Hanson GT: Cell-based potassium ion channel screening using the FluxOR assay. *J Biomol Screen* 2010;15:441–446.
41. Zhang XF, Zhang D, Surowy CS, *et al.*: Development and validation of a medium-throughput electrophysiological assay for KCNQ2/3 channel openers using QPatch HT. *Assay Drug Dev Technol* 2013;11:17–24.
42. Yue JF, Qiao GH, Liu N, Nan FJ, Gao ZB: Novel KCNQ2 channel activators discovered using fluorescence-based and automated patch-clamp-based high-throughput screening techniques. *Acta Pharmacol Sin* 2016;37:105–110.
43. Jow F, Shen R, Chanda P, *et al.*: Validation of a medium-throughput electrophysiological assay for KCNQ2/3 channel enhancers using IonWorks HT. *J Biomol Screen* 2007;12:1059–1067.
44. Fritch PC, McNaughton-Smith G, Amato GS, *et al.*: Novel KCNQ2/Q3 agonists as potential therapeutics for epilepsy and neuropathic pain. *J Med Chem* 2010;53:887–896.
45. Finkel A, Wittel A, Yang N, Handran S, Hughes J, Costantin J: Population patch clamp improves data consistency and success rates in the measurement of ionic currents. *J Biomol Screen* 2006;11:488–496.
46. Wickenden AD, Zou A, Wagoner PK, Jegla T: Characterization of KCNQ5/Q3 potassium channels expressed in mammalian cells. *Br J Pharmacol* 2001;132:381–384.
47. Cheung YY, Yu H, Xu K, *et al.*: Discovery of a series of 2-phenyl-N-(2-(pyrrolidin-1-yl)phenyl)acetamides as novel molecular switches that modulate modes of K(v)7.2 (KCNQ2) channel pharmacology: identification of (S)-2-phenyl-N-(2-(pyrrolidin-1-yl)phenyl)butanamide (ML252) as a potent, brain penetrant K(v)7.2 channel inhibitor. *J Med Chem* 2012;55:6975–6979.
48. Bock C, Link A: How to replace the lost keys? Strategies toward safer KV7 channel openers. *Future Med Chem* 2019.
49. Tatulian L, Brown DA: Effect of the KCNQ potassium channel opener retigabine on single KCNQ2/3 channels expressed in CHO cells. *J Physiol* 2003;549(Pt 1):57–63.
50. Zhou P, Yu H, Gu M, Nan FJ, Gao Z, Li M: Phosphatidylinositol 4,5-bisphosphate alters pharmacological selectivity for epilepsy-causing KCNQ potassium channels. *Proc Natl Acad Sci U S A* 2013;110:8726–8731.
51. Blom SM, Schmitt N, Jensen HS: Differential effects of ICA-27243 on cloned K(V)7 channels. *Pharmacology* 2010;86:174–181.

Address correspondence to:
Benjamin Wilenkin, MS
Department of Quantitative Biology
Eli Lilly and Company
355 E Merrill St
Indianapolis, IN 46225

E-mail: wilenkin_benjamin_s@lilly.com

Abbreviations Used

CHO = Chinese hamster ovary
CI = confidence interval
DMSO = dimethyl sulfoxide
DRG = dorsal root ganglion
EGTA = ethylene glycol-bis(2-aminoethylether)-N,N,N′,N′,-tetraacetic acid
GABA = gamma-aminobutyric acid
HEPES = 2-[4-(2-hydroxyethyl)piperazin-1-y]ethanesulfonic acid
IWB = Ionworks Barracuda
PPC = population patch clamp
SARs = structure-activity relationships
SD = standard deviation
SEM = standard error of the mean